Solution Structure of a Platelet Receptor Peptide Bound to Bovine α-Thrombin†

Feng Ni,*,‡ Daniel R. Ripoll,‡ Philip D. Martin,§ and Brian F. P. Edwards§

Biotechnology Research Institute, National Research Council of Canada, 6100 Royalmount Avenue, Montréal, Québec, Canada H4P 2R2, and Department of Biochemistry, Wayne State University, Detroit, Michigan 48201

Received June 10, 1992; Revised Manuscript Received August 17, 1992

ABSTRACT: NMR experiments were carried out to study the interaction of thrombin with a synthetic peptide, ESKATNATLDPR, derived from the newly-identified platelet receptor for thrombin [Vu, T.-K. H., Hung, D. T., Wheaton, V. I., & Coughlin, S. R. (1991) *Cell 64*, 1057–1068]. On the basis of the observation of the thrombin-induced line broadening and transferred NOEs, binding of the peptide was found to be located exclusively within residues LDPR of the proteolytic cleavage site LDPR/S essential for receptor activation by thrombin. Measurement of transferred NOEs and molecular modeling indicate that the side chain of the Asp(P_3) residue may form a hydrogen bond with thrombin and, by doing so, it is brought near a positively-charged thrombin residue Arg(221A), thereby partially neutralizing the negative charge of an Asp residue at this site of protein substrates. The hydrophobic side chains of residues Leu(P_4) and Pro(P_2) reside on the same side of the peptide backbone as indicated by transferred NOEs and were found by modeling to fit into a hydrophobic cage around the thrombin active site. These results suggest that the interaction of thrombin with protein substrates such as prothrombin, protein C, protein S, the platelet receptor, and the Aα- and Bβ-chains of fibrinogen all follow the same canonical binding mode in that the substrate forms an antiparallel β-strand with thrombin. For optimal interaction, thrombin requires bulky hydrophobic residues at the P_2 and P_4 sites on the substrate, and in the case of fibrinopeptide A where the P_4 residue is a Gly without a side chain, distant Phe(P_9) and Leu(P_8) residues are brought back by unique structural elements to occupy the S_4 specificity pocket near the active site of thrombin [Ni, F., Meinwald, Y. C., Vasquez, M., & Scheraga, H. A. (1989) *Biochemistry 28*, 3094–3105; Martin P. D., Robertson, W., Turk, D., Huber, R., Bode, W., & Edwards, B. F. P. (1992) *J. Biol. Chem. 267*, 7911–7920].

Thrombin is a trypsin-like serine protease generated as an end-product of the zymogen activation cascade in blood coagulation (Fenton, 1981). Its primary function is to convert the soluble fibrinogen into the fibrin clot. It amplifies its own generation by activating clotting factors V and VIII. It stimulates platelet aggregation and activates the fibrin cross-linking factor XIII. Thrombin also binds to thrombomodulin and activates protein C, initiating the natural anticoagulant pathway (Esmon, 1989).

Since the cloning of a platelet thrombin receptor, it has been established that both the active site and the fibrinogen-binding exosite of thrombin are involved in the recognition of the platelet receptor by thrombin (Vu et al., 1991a,b). Thrombin activation of the platelet receptor is reminiscent of the thrombin–fibrinogen interaction. In both cases, an NH_2-terminal extension of the protein is released by thrombin cleavage, exposing a new NH_2 terminus which is responsible for subsequent events. The thrombin–fibrinogen interaction leads to fibrin polymerization (Laudano & Doolittle, 1978). The thrombin receptor interaction activates platelets leading to platelet aggregation (Vu et al., 1991a,b). Active-site mapping and NMR[1] studies revealed that the specificity of thrombin toward the Aα chain of fibrinogen is determined in part by the unique structural features of fibrinogen near the cleaved Arg–Gly peptide bonds (Ni et al., 1989a,b; Zheng et al., 1992). It is possible that the thrombin recognition of the platelet receptor follows a similar mechanism, requiring as many as 10 residues N-terminal to the cleavage site LDPR/S, identified on the basis of sequence homology to other proteins such as protein C or protein S (Vu et al., 1991a). We have carried out NMR-transferred NOE studies in order to establish the structure of platelet receptor peptides in the thrombin-bound state. Our results confirm the assignment of LDPR as the minimal binding sequence for the thrombin–receptor interaction.

MATERIALS AND METHODS

Sample Preparation. The platelet receptor peptide Ac-Glu(30)-Ser-Lys-Ala-Thr-Asn-Ala-Thr-Leu(38)-Asp(39)-Pro(40)-Arg(41)-COOH was synthesized on an ABI/430a peptide synthesizer (Applied Biosystems). The purified peptide had an amino acid composition of Asx 1.95 (2.0), Thr 1.80 (2.0), Ser 0.84 (1.0), Glx 0.95 (1.0), Ala 2.00 (2.0), Leu 1.01 (1.0), Lys 1.01 (1.0), Arg 0.92 (1.0), Pro 1.02 (1.0) and an observed molecular weight of 1343.9 (1343.7). Bovine α-thrombin was prepared as described previously (Ni et al., 1990). Weighed amounts (10 mg) of the peptide (content 77% + salted water) were dissolved in 500 μL of an NMR solution that was 150 mM NaCl, 50 mM sodium phosphate, and 0.2 mM EDTA at pH 5.3. A volume of 100 μL of the corresponding D_2O solution was added to provide the deuterium lock signal for the NMR spectrometer. The final pH of the peptide solution was adjusted to 5.3 with the use of dilute NaOH or HCl solutions to slow down the autolysis of thrombin (Ni et al., 1989a). For a sample of the free peptide, 300 μL of the peptide was mixed with 200 μL of the NMR solution before transfer to the NMR tube. For a sample of the peptide–thrombin complex, the NMR solution was replaced with 200 μL of a stock solution (37 mg/nL at pH

† NRCC Publication No. 33105. This work was supported in part by Ciba-Geigy Canada Ltd. and by NIH Grant GM33192 (B.F.P.E.).

* To whom correspondence should be addressed.

‡ National Research Council of Canada.

§ Wayne State University.

[1] Abbreviations: NMR, nuclear magnetic resonance; NOE, nuclear Overhauser effects; NOESY, two-dimensional nuclear Overhauser and exchange spectroscopy; COSY, *J*-correlated spectroscopy; EDTA, ethylenediaminetetraacetic acid; FpA, fibrinopeptide A.

0006-2960/92/0431-11551$03.00/0

Table I: Proton Resonance Assignments of the Receptor Peptide in Aqueous Solution at 15 °C

residue	chemical shift[a] (ppm)			
	NH	αCH	βCH	others
E30	8.48	4.30	1.97, 2.08	γCH_2 2.33
S31	8.59	4.49	3.88, 3.93	
K32	8.49	4.38	1.80, 1.90	γCH_2 1.48; δCH_2 1.71; ϵCH_2 3.03
A33	8.43	4.41	1.44	
T34	8.27	4.35	4.27	γCH_3 1.24
N35	8.52	4.75	2.81, 2.89	
A36	8.39	4.39	1.44	
T37	8.24	4.33	4.23	γCH_3 1.24
L38	8.29	4.40	1.66, 1.66	γCH 1.64; δCH_3 0.89, 0.95
L38[b]	?	?	?	γCH ?; δCH_3 0.07, −0.17
D39	8.40	4.88	2.53, 2.78	
D39[c]	7.98	4.77	2.49, 2.67	
P40		4.48	2.07, 2.27	γCH_2 2.07; δCH_2 3.77, 3.84
P40[c]		?	?	γCH_2 1.98; δCH_2 3.52, 3.63
R41	8.10	4.16	1.77, 1.89	γCH_2 1.67; δCH_2 3.24; εNH 7.35
R41[c]	8.34	4.20	?	γCH_2 ?; δCH_2 3.24; εNH 7.26

[a] The chemical shift values were calibrated against the solvent proton resonance that was set to 4.80 ppm at 25 °C. The undetermined values are indicated by a question mark. [b] The chemical shifts are those of Leu(38) in the thrombin-bound state. [c] These resonances are those of the corresponding residues of the receptor peptide when Pro(40) is in the cis conformation.

5.3) of bovine α-thrombin. The final concentration of the peptide was 5.7 mM, and that of thrombin was 0.4 mM.

NMR Experiments and Molecular Modeling. All NMR experiments were carried out on a Brüker AM-500 MHz spectrometer using procedures described in our previous work (Ni et al., 1990, 1992; Ni, 1992b). Sequence-specific assignments of the proton resonances (Table I) were established using standard procedures (Wüthrich, 1986) by an analysis of the cross-peak patterns in a double-quantum-filtered COSY and a transferred NOE spectrum of the peptide in the presence of thrombin.

The dissociation rate constant k_{off} of the peptide from the complex was calculated from the exchange broadening of the peptide resonances in the thrombin-bound state. If the exchange rate is slow on the scale of the chemical shift separation, the bound resonances of the peptide are broadened by an amount equal to the rate of exchange (Jardetzky & Roberts, 1981):

$$\pi\Delta\nu_B = 1/T_{2B} + k_{off}$$

where $\Delta\nu_B$ is the measured line width of a resonance of the bound peptide and T_{2B} is the transverse relaxation rate of the bound resonance in the absence of exchange. In the current work, the intrinsic linewidth $\Delta\nu = 1/\pi T_{2B}$ of the bound peptide was assumed to be equal to the average line width of the resolved resonances from the thrombin molecule (Ni et al., 1990). All line width measurements were made from a one-dimensional slice along the F_1 direction of the transferred NOESY spectra of the peptide.

Distance geometry computations were carried out using the program DGEOM (Blaney et al., 1990) obtained through the Quantum Chemistry Program Exchange at Indiana University. Energy minimizations were carried out using the force field provided by the software program Sybyl (Tripos) with all protons considered explicitly. For the thrombin–peptide complex, energy minimization included only residues within a sphere of 12-Å radius from the C^α atom of Arg(41) of the peptide. A set of approximate NOE distances were incorporated as RANGE constraints. The constraints also included the hydrogen bond between the backbone NH atom of Arg(41) of the peptide and the carbonyl oxygen of Ser-(214) of thrombin and the two antiparallel β-sheet hydrogen bonds between Asp(39) of the peptide and Gly(216) of thrombin that were observed in the crystal structure of anFpA–thrombin complex (Martin et al., 1992).

Initial interproton distances were estimated from two-dimensional transferred NOE spectra obtained at a temperature of 15 °C with mixing times ranging from 50 to 500 ms. The relative intensities of the NOE cross-peaks were classified into three categories, strong, medium, and weak with upper distance bounds of 3.0 Å, 3.6 Å, and 4.2 Å, respectively, in reference to the various NOEs between the protons in the ring of Pro(40) (Ni et al., 1990). An upper bound was relaxed to 4.5 Å if the observed NOE was extremely weak, but still identifiable. The approximate NOE distances were further refined by use of an iterative technique. This involved the calculation of the theoretical transferred NOEs expected from a model complex under the experimental conditions. The calculated spectra were inspected to identify cross-peaks that were absent experimentally or cross-peaks that had grossly different NOE intensities. Protons with weaker (or missing) experimental NOEs were pushed apart by incrementing the distance constraints during subsequent constrained energy minimization. Otherwise, they are pulled together by decrementing the distances.

Theoretical transferred NOEs were calculated using an extended procedure for the complete relaxation matrix analysis of multispin exchanging systems (Ni, 1992a). Only selected residues of the enzyme were considered during simulation of transferred NOEs. These included residues His(57), Tyr-(60A), Trp(60D), Leu(99), Ile(174), Asp(189)–Ser(195), Val-(213)–Cys(220), Arg(221A), and Gly(226) that constitute the catalytic active site of bovine thrombin (Martin et al., 1992). The enzyme protons in both the free and bound states were taken into account in addition to an explicit consideration of the ligand off-rate. The tumbling correlation time for the thrombin–peptide complex was taken to be 20 ns expected for a globular protein of molecular mass 40 kDa (Cantor & Schimmel, 1980). A short correlation time of 0.5 ns was assumed for the peptide in accordance with the close-to-null NOEs observed for the free peptide. The internal dynamics of the methyl groups was treated using a jump model (Woessner, 1962, 1965; Tropp, 1980) with a correlation time of 25 ps. The simulation utilized a leakage relaxation rate of 0.2 s^{-1} for the free peptide and 2 s^{-1} for both thrombin and the thrombin–peptide complex. The dissociation constant for the complex was set to 1 mM estimated on the basis of the K_m of 0.9 mM for the peptide substrate PESKATNATLD-PRSFLL (Vu et al., 1991b) and the K_i of 0.96 mM for a related peptide inhibitor, LDPRPFLL (Liu et al., 1991). The calculation also included the effects of short recycle times (1.67–2.17 s in NOE experiments) to account for intensity attenuations associated with slowly-relaxing protons (Eaton & Andersen, 1987).

RESULTS

Differential Line Broadening in the Receptor Peptide. Figure 1 shows the NH region of the proton NMR spectra of the receptor peptide in the absence (1A) and in the presence (1B) of bovine α-thrombin. It is seen that some peaks are more affected by thrombin binding than others. The NH peaks of Leu(38) and Arg(41) are significantly broadened while the broadening on the NH peak of Thr(37) is less severe (Figure 1B). On the other hand, thrombin has minimal effects on the NH peaks of Glu(30) [and/or Lys(32)], Ser(31), Ala-(33), Thr(34), and Asn(35). Since line broadening effects

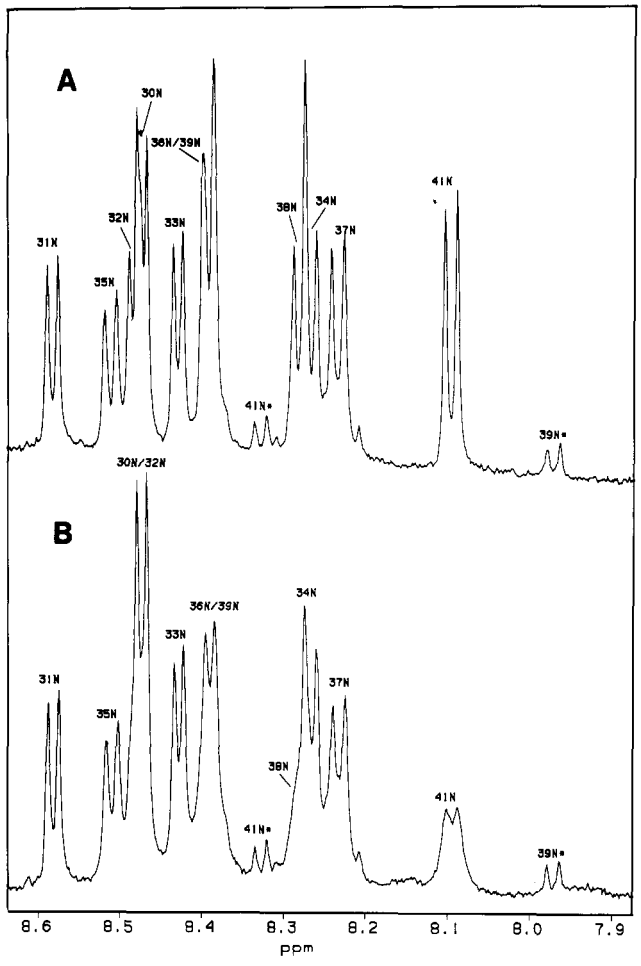

FIGURE 1: NH regions of the proton NMR spectra of the free receptor peptide (A) and the peptide in the presence of thrombin (B). The spectra were acquired with a peptide concentration of 5.7 mM and a thrombin concentration of 0.4 mM at 15 °C. The minor resonances (*) are the result of the cis–trans isomerization of Pro(40) (Table I).

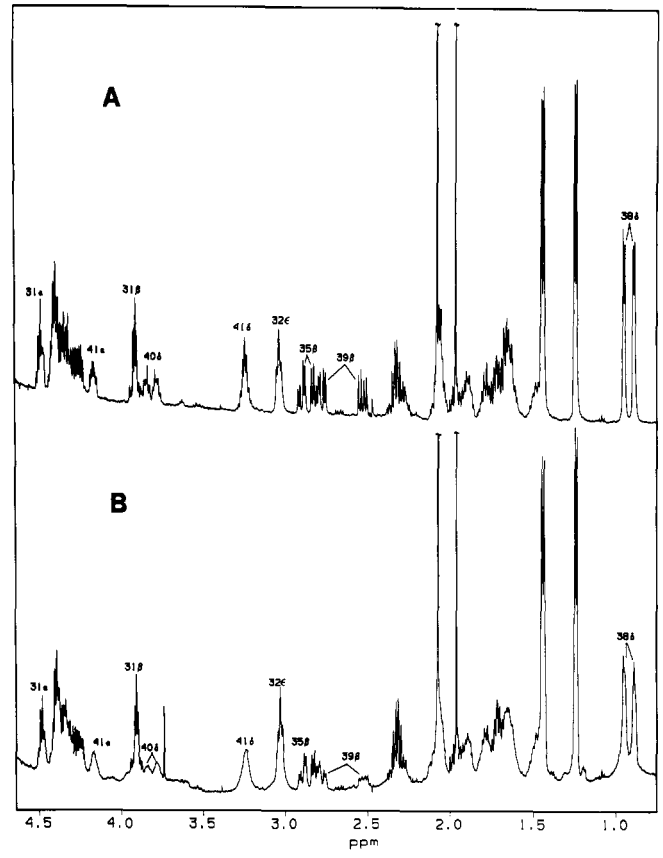

FIGURE 2: αCH and the side-chain proton resonances of the receptor peptide in the absence (A) and the presence (B) of thrombin. The experimental conditions were the same as those indicated in Figure 1. Note the differential line broadening on the resonances of Leu-(38), Asp(39), Pro(40), and Arg(41).

diminish from Thr(37) to Glu(30), we can assume that the sharp peaks at the NH resonance position of residues Ala(36) and Asp(39) are primarily from the NH proton of Ala(36). Thus, the NH proton of Asp(39) may also be greatly broadened by thrombin binding. In correlation with NH line broadening, there is also broadening on the side-chain proton resonances of Leu(38), Asp(39), Pro(40), and Arg(41) (Figure 2). The NMR spectrum of the peptide in the presence of thrombin represents an average behavior of the free peptide and the peptide in the thrombin-bound state. To a first approximation, the differential line broadening can be attributed to the differential mobility of the peptide residues in the thrombin-bound state (Ni et al., 1989a). Therefore, residues Glu(30) to Thr(37) of the peptide may be more mobile than residues Leu(38) to Arg(41) in the thrombin–peptide complex.

The differential mobilities of the peptide residues were further investigated by following the buildup of the resolved transferred NOEs between adjacent residues. While the magnitudes of the sequential $d_{\alpha N}$ NOEs for residues Glu(30) to Thr(37) continue to increase up to an NOE mixing time of 500 ms, there are already significant decays at 350 ms for the corresponding NOEs between residues Leu(38) and Asp-(39) and between Pro(40) and Arg(41). There are similar decays for the intraresidue NOEs between the NH and βCH or the αCH and βCH protons of residues Leu(38), Asp(39), Pro(40), and Arg(41). This kind of NOE decay usually indicates an increased extent of spin diffusion (Keepers & James, 1984; Olejniczak et al., 1986) which may be a result of the binding of these residues to thrombin. Importantly, the $d_{\alpha N}$ $(i, i+1)$, $d_{N\beta}$ (i, i), and/or $d_{\alpha\beta}(i, i)$ NOE intensities continuously decrease toward the NH_2 terminus of the peptide starting from residue Thr(37) such that only NOEs pertaining to residues Ala(36) to Arg(41) are present at short mixing times (Figure 3). The diminished NOEs for residues Glu-(30) to Asn(35) are in good agreement with the line broadening effects, suggesting that thrombin binding may greatly restrict the mobility of residues Leu(38) to Arg(41) while residues Glu(30) to Asn(35) tumble in similar ways as in the free peptide. Residues Ala(36) and Thr(37) exhibit intermediate mobilities as expected for a segment connecting the fast-moving ESKATN to the binding sequence LDPR which are tightly embedded in the active site of thrombin.

It is interesting to note that thrombin does not affect the minor NH resonance signals which were assigned to the NH protons of Asp(39) and Arg(41) in the cis population of Pro-(40) of the peptide (Figure 1). Furthermore, no transferred NOEs were detected between the proton resonances which originate from residues Asp(39), Pro(40), and Arg(41) of the peptide when Pro(40) is in the cis conformation (Table I). These observations suggest that thrombin does not bind to the peptide if Pro(40) is in a cis conformation, in agreement with the previous finding that thrombin binds only to the trans Pro population of a substrate analog acetyl-D-Phe-Pro-Arg-Gly (DiMaio et al., 1991).

Transferred NOEs and Exchange Kinetics of the Thrombin–Peptide Complex. In the presence of thrombin, the LDPR segment of the receptor peptide exhibits a significant amount of NOE cross-peaks which otherwise were absent for the free

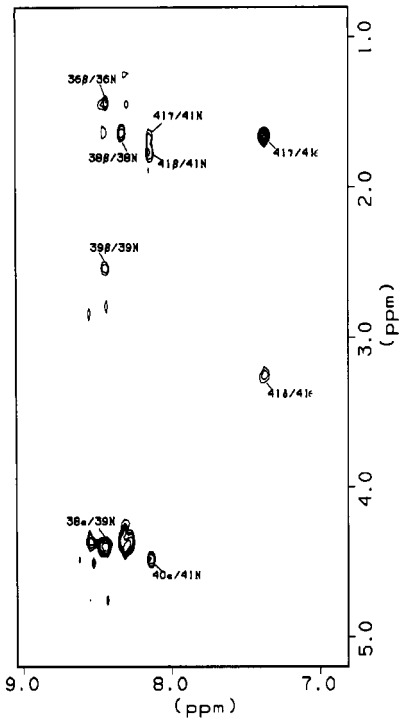

FIGURE 3: Transferred NOEs of the receptor peptide at a short mixing time of 50 ms. The sample is the same as that used in Figures 1B and 2B. The NOESY spectrum was acquired with a postacquisition delay of 2.17 s at a temperature of 15 °C. The resonance assignments are documented in Table I. The label, 40α/41N, for example, indicates the sequential NOE between the αCH proton of Pro(40) and the NH proton of Arg(41).

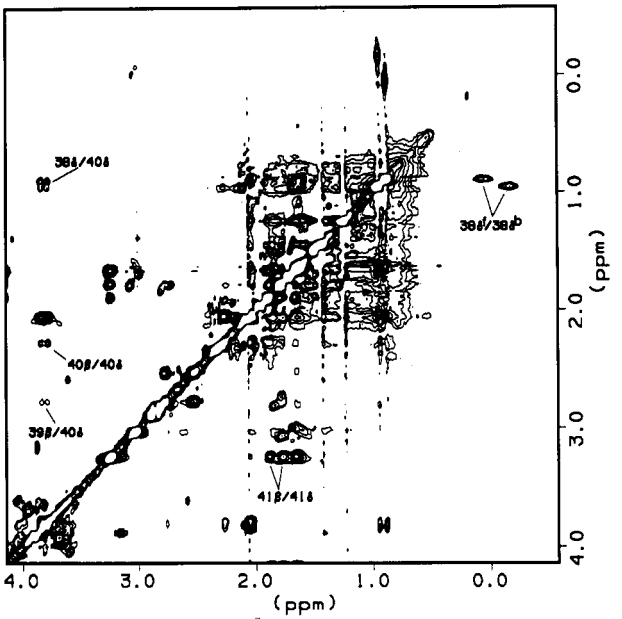

FIGURE 4: Transferred NOEs involving the side-chain protons of the peptide. The spectrum was obtained with a mixing time of 200 ms under the same experimental conditions as those in Figure 3. Note the cluster of four peaks (38δ/40δ) involving the δCH protons of residues Leu(38) and Pro(40). The broad cross-peaks (38δ^f/38δ^b) are due to the exchange between the δCH_3 proton resonances of Leu(38) from the free and bound peptides (see the text for details).

peptide in aqueous solution. Particularly, there are strong sequential $d_{\alpha N}$ connectivities between rsidues Leu(38) and Asp(39) and between residues Pro(40) and Arg(41) (Figure 3) and $d_{\alpha\delta}$ NOEs between Asp(39) and Pro(40) (not shown). There are, however, no d_{NN} connectivities from residue Thr(37) to Asp(39). Furthermore, there are weak NOEs between one of the βCH_2 protons of Asp(39) and the δCH_2 protons of Pro(40) (Figure 4). There are also transferred NOEs between the δCH protons of Leu(38) and Pro(40), indicating that the side chains of the two residues pack together on the same side of the peptide backbone.

Apart from transferred NOEs, the NOESY spectra of the peptide–thrombin complex consistently contained cross-peaks to a spectral region (~0 ppm) free from peptide signals (Figure 4). These cross-peaks originate from the two δCH_3 proton resonances of Leu(38) of the free peptide and exhibit significantly broadened line shapes compared to transferred NOE cross-peaks. Upon an increase in temperature, there is a significant loss in the intensity of the cross-peaks due to further broadening of the bound signals (spectra not shown). These observations indicate as exchange phenomenon between the well-separated free and bound δCH_3 proton resonances of Leu(38) and suggest that the thrombin–peptide complex follows a slow binding behavior on the time scale of the chemical shift separation (Jardetzky & Roberts, 1981). Specifically, an 0.8 ppm (400 Hz) separation between the free and bound δCH_3 proton resonances of Leu(38) places an upper bound of 400 s^{-1} for the off-rate (k_{off}) of the peptide from the complex. An estimate of 160–220 s^{-1} for k_{off} at 15 °C and 250–310 s^{-1} at 25 °C were obtained from the exchange broadening of ~60 Hz and ~90 Hz at 15 °C and 25 °C, respectively.

Solution Structure of the Thrombin–Peptide Complex. The bound structure of LDPR was investigated by iterative model building combining the NMR data with X-ray structural information. An initial model of LDPR was constructed from the GGVR portion of FpA in the thrombin–FpA complex (Martin et al., 1992). The side chain of Leu(38) was rotated from the gauche$^-$ ($\chi_1 = -60$) to the trans conformation ($\chi_1 = 180$) to avoid bad contacts with the side chain of Ile(174) of thrombin. Theoretical transferred NOEs were then calculated with a ligand k_{off} of 200 s^{-1} along with other parameters specified in the Materials and Methods section. The initial model contained an extended structure and produced a theoretical spectrum in close resemblance with experimental NOEs involving residues Asp(39), Pro(40), and Arg(41). The agreement between the predicted and the observed NOEs suggests that Arg(41) binds to the S_1 pocket of thrombin in a very similar conformation as Arg(P_1) of fibrinopeptide A in the crystal structure.

A close inspection of the theoretical spectrum revealed that the initial model does not reproduce the transferred NOEs between the side-chain protons of Leu(38) and Pro(40) (Figure 4). Furthermore, the patterns of the computed intraresidue NOEs between the NH and the side-chain protons of Leu(38) did not match those in the experimental spectra. These NOE differences indicate that the side-chain conformation of Leu(38) may not be correctly assigned in the starting model. The refinement steps thus included some NOE distance bounds during a constrained energy minimization of the thrombin–peptide complex. The new structure models were again used to calculate theoretical transferred NOEs. At each step of the refinement, the NOE distances were updated on the basis of the identification of mismatched NOE cross-peaks (see the Materials and Methods section).

Further refinements involved the use of distance geometry so that a more complete set of conformations of the peptide can be found that match the updated set of NOE distances (Table II). All of the converged conformations contain an extended structure with an almost unique packing orientation of the side chain of Leu(38) against Pro(40) (Figure 5). The Arg side chain also clusters around a single orientation which

Table II: Refined Interproton Distances for the Thrombin-Bound Receptor Peptide[a]

L38–L38	HN–HB1 2.6, 3.0; HN–HB2 2.6, #; HN–HG 2.6, #; HN–HD11 3.6, 4.2; HN–HD12 3.6, #; HN–HD13 3.6, #; HN–HD21 3.6, #; HN–HD22 3.6, #; HN–HD23 3.6, 4.2; HA–HG 3.2, #; HA–HD1 3.2, #; HA–HD2 3.2, #
D39–D39	HN–HB2 1.8, 2.6
R41–R41	HN–HB1 1.8, 2.6; HN–HG1 2.6, #; HN–HG2 2.6, 3.2; HN–HD1 3.6, 4.2; HN–HD2 3.6, #; HN–HE 4.0, #; HA–HG1 1.8, 2.6; HA–HD 4.0, #; HA–HE 4.0, #; HB–HD 1.8, 2.6; HB–HE 4.0, #; HG–HE 1.8, 2.6
L38–D39	HA–HN 1.8, 2.6; HA–HA 4.0, #; HB2–HN 1.8, 2.6; HD12–HN 3.6, 4.0; HD23–HN 3.6, 4.5; HN–HN 4.0, #
D39–P40	HB1–HD2 3.6, 4.0; HB2–HD2 4.0, #; HN–HD1 3.6, 4.0; HN–HD2 4.0, #; HA–HA 4.0, #
P40–R41	HA–HN 1.8, 2.6; HB–HN 2.6, 3.2; HD–HN 4.0, #; HA–HA 4.0, #; HA–HD1 3.0, 4.5; HA–HD2 3.6, #; HA–HB1 3.6, 4.0; HA–HB2 3.6, #; HA–HG1 3.2, #; HA–HG2 3.2, 3.6
L38–P40	HD21–HA 3.6, 4.0; HD1–HB 4.0, #; HD2–HB 4.0, #; HD12–HG2 2.6, 3.2; HD21–HG2 2.6, 3.2; HG–HD 4.0, #; HB–HD 4.0, #; HD11–HD1 3.6, #; HD12–HD1 2.9, 3.1; HD23–HD1 3.6, #; HD21–HD1 2.9, 3.1
D39–R41	HB–HE 4.0, #

[a] The pair of numbers represents the lower and upper bounds of the corresponding interproton distance. The # sign indicates that the upper bound is unconstrained during energy minimization or distance geometry calculations. No prochiral assignments were implied by the specific names of all the protons. Therefore, the chiralities of the prochiral centers were allowed to "float" during distance geometry calculations (Blaney et al., 1990).

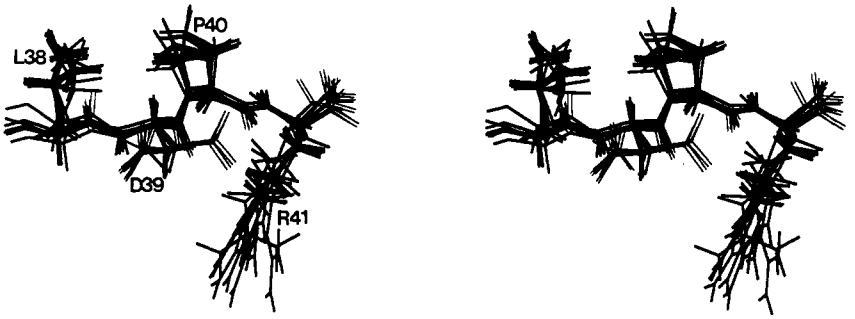

FIGURE 5: Cluster of distance geometry structures of the peptide fragment LDPR. The superposition was carried out using the C^{α} and C^{β} atoms of each residue. No prochiral assignments were assumed during the distance geometry calculations (see Table II). This is seen with Asp(39) where both the gauche$^-$ ($\chi_1 = -60$) and the gauche$^+$ ($\chi_1 = 60$) conformations were allowed for the side-chain orientations. But only a gauche$^-$ ($\chi_1 = -60$) conformation for Asp(39) is supported by the NMR data (see the text). The structures presented here were also refined by a constrained energy minimization of the free peptide.

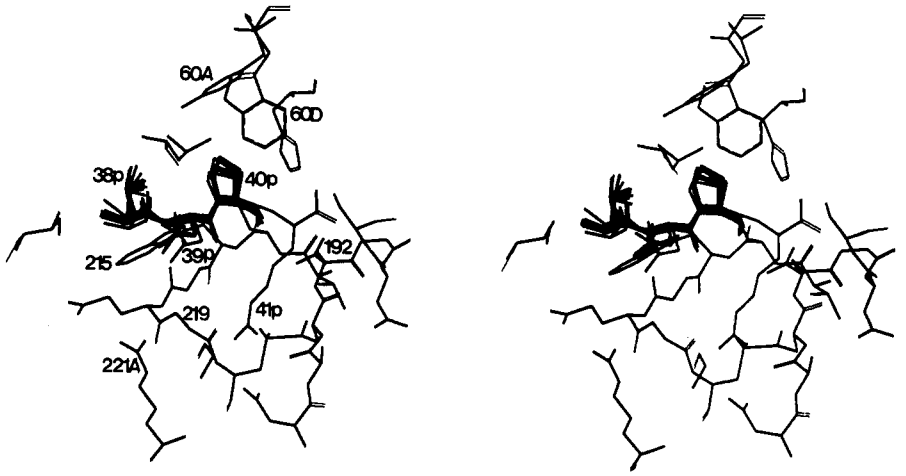

FIGURE 6: Model structure of the thrombin–LDPR complex. The peptide residues are indicated as 38p, 39p, 40p, and 41p. Superimposed are also residues Leu(38), Asp(39), and Pro(40) from the distance geometry structures of LDPR in Figure 5 with gauche$^-$ ($\chi_1 = -60$) conformation for the Asp residue.

would project into the active site of thrombin. The Asp(39) side chain, on the other hand, is populated around two discrete conformers: gauche$^-$ ($\chi_1 = -60$) and gauche$^+$ ($\chi_1 = +60$). This is due to the fact that the chiralities of the prochiral centers were allowed to "float" during distance geometry calculations (Blaney et al., 1990) to allow for the absence of stereospecific assignments (Table II). However, the gauche$^+$ conformer would be unfavorable energetically since the side-chain carboxylate group of Asp(39) stacks against the backbone carbonyl oxygen and the carbonyl oxygen of the next residue Pro(40) (Figure 5). A further analysis of the spectrum of the peptide (Figure 2A) revealed that the more upfield shifted of the two βCH_2 protons of Asp(39) has a larger coupling constant (8.35 Hz) to the αCH proton than that (6.09 Hz) of the downfield one. This indicates that the upfield peaks should be assigned to the *pro-R* βCH proton (Ni et al., 1992). Given the fact that it is this upfield-shifted proton that has a stronger transferred NOE to the NH proton of Asp(39) (Figure 3), the gauche$^-$ conformation of Asp(39) should be the preferred side-chain orientation in the thrombin-bound state.

The refined NOE distances (Table II) were subsequently included in the final refinement of the complex structure adopting a gauche$^-$ conformation for the Asp(39) side chain. The new structure predicted the almost equal intensities of the transferred NOEs between the two resolved methyl protons of Leu(38) and the δCH_2 protons of Pro(40) (Figure 4). Furthermore, there is an almost perfect superposition between

Table III: Primary Sequences of Protein Substrates That Are Cleaved by Thrombin[a]

	P_9	P_8	P_7	P_6	P_5	P_4	P_3	P_2	P_1
receptor	A	T	N	A	T	L	D	P	R
receptor (hamster)	M	T	D	A	T	V	N	P	R
protein C	D	Q	E	D	Q	V	D	P	R
protein C (bovine)	D	Q	K	D	Q	L	D	P	R
factor V	T	H	H	A	P	L	S	P	R
factor VIII	S	K	N	N	A	I	E	P	R
prothrombin	Q	V	T	V	A	M	T	P	R
prothrombin (bovine)	R	V	T	V	E	V	I	P	R
factor XIII	V	E	L	Q	G	V	V	P	R
protein S	S	T	N	A	Y	P	D	L	R
factor XI	E	C	T	T	K	I	K	P	R
fibrinopeptide B	N	E	E	G	F	F	S	A	R
fibrinopeptide A (lamprey)				D	D	I	S	L	R
fibrinopeptide A	F	L	A	E	G	G	G	V	R

[a] Protein sequences were taken from the following sources: receptor, Vu et al. (1991a); receptor (hamster), Rasmussen et al. (1991); protein C and protein C (bovine), Kiesel and Davie (1981); factor V, Jenny et al. (1987); factor VIII, Vehar et al. (1984); prothrombin, Degen et al. (1983); prothrombin (bovine), MacGillivray and Davie (1984); factor XIII, Ichinose et al. (1986); protein S, Dahlback et al. (1986); factor XI, Fujikawa et al. (1984); fibrinopeptide B, Furlan (1988); fibrinopeptide A (lamprey), Martin et al. (1992); fibrinopeptide A, Ni et al. (1989a).

the LDPR peptide structure in the complex and the ensemble of LDPR conformations sampled by distance geometry (Figure 6). The side chains of both Leu(38) and Pro(40) stack against the aromatic rings of residues Tyr(60A), Trp(60D), and Trp-(215) near the thrombin active site. Such a spatial arrangement would explain the dramatic upfield shift of the δCH_3 proton resonances of Leu(38) for the peptide in the thrombin-bound state (Figure 4 and Table I). More interestingly, the side chain of Asp(39) can form a hydrogen bond with the amide nitrogen of Gly(219) on thrombin so that the Asp side chain is oriented by a gauche$^-$ ($\chi_1 = -60$) conformation toward the positively-charged residue Arg(221A) of thrombin (Figure 6). This fixed conformation would greatly reduce the mobility of the Asp side chain in agreement with the thrombin-induced line broadening on the βCH_2 proton resonances of Asp(39) (Figure 2).

DISCUSSION

On the basis of the sequence homology with protein C, the peptide segment LDPR/S in the platelet receptor has been identified as the recognition sequence for the thrombin active site (Vu et al., 1991a). Site-directed mutagenesis experiments indicated that LDPR is essential for the thrombin cleavage of the platelet receptor (Vu et al., 1991b). It was also shown that thrombin cleaves the receptor peptide PESKATNATLD-PR/SFLL with a K_m of 0.9 mM. Furthermore, a related peptide LDPRPFLL was found to inhibit the catalytic activity of thrombin with a K_i of 0.96 mM (Liu et al., 1991). These results suggest that residues Pro(29) to Thr(37) might not contribute significantly to the interactions of the platelet receptor with thrombin. The NMR data obtained in the present study provide the first structural evidence for the involvement of the receptor residues LDPR in the interaction with thrombin. Residues 30–37 of the receptor peptide are exposed to the solvent in the thrombin–peptide complex and have no significant contacts with thrombin. Residues LDPR, on the other hand, interact with thrombin even after thrombin cleavage, producing a thrombin–product complex that has reasonable stability ($k_{off} \sim 200\ s^{-1}$). Table III lists some of the primary sequences N-terminal to the thrombin cleavage sites in various protein substrates. It is seen that the P_4 subsite is occupied almost exclusively by hydrophobic residues and the P_2 subsite is occupied by Pro residues. The residues preceding the P_4 residue, on the other hand, show great sequence variation. These data suggest that thrombin may interact with residues P_1–P_4 of all the protein substrates through a canonical antiparallel β-strand as shown in Figure 6. In such a structure of the complex, the hydrophobic side chains of the P_2 and P_4 residues would interact favorably with the highly hydrophobic cage around the thrombin active site. In the case of human fibrinopeptide A, on the other hand, the missing hydrophobic side chain at the P_4 site is replaced by the side chains of distant Phe(P_9) and Leu(P_8) residues which are brought back by unique structural elements to occupy the S_4 specificity pocket at the active site of thrombin (Ni et al., 1989b; Martin et al., 1992).

It has been suggested recently that the negatively-charged aspartice residue in the P_3 position is responsible for the slow activation of protein C by thrombin. Detailed kinetic analysis indicated that this Asp residue has some influence on the turnover rate k_{cat} but shows negligible effect on the binding constant K_m (Ehrlich et al., 1990; Le Bonniec et al., 1991; Le Bonniec & Esmon, 1991). Furthermore, Asp, Glu, or other polar residues have high occurrences at the P_3 subsite of many protein substrates of thrombin (Table III). These observations support the conclusion that thrombin can accommodate negatively-charged residues Asp(P_3) or Glu(P_3) in the Michaelis enzyme–substrate complex despite the possibility that Asp or Glu might interact unfavorably with the negatively-charged thrombin residue Glu(192) (Le Bonniec & Esmon, 1991). The structural model for the thrombin–peptide complex indicates that the carboxylate group of Asp may form a hydrogen bond with the amide nitrogen of residue Gly(219) on thrombin (Figure 6). By doing so, the Asp side chain is brought close to the positively-charged Arg(221A) of thrombin, thereby partially neutralizing the negative charge of an Asp(P_3) residue at this site of substrates. The structural model may also account for the tolerance of other polar residues such as Asn, Ser, or Thr at the P_3 subsite of protein substrates (Table III). Like Asp, these residues all have the capability to form side-chain to main-chain hydrogen bonds between the substrate and the enzyme such as the one illustrated in Figure 6. It is interesting to note that thrombin also cleaves factor XI at the recognition sequence IKPR/I (Naito & Fujikawa, 1991; Fujikawa et al., 1986). The positively-charged Lys-(P_3) may adopt a side-chain conformation different from that of Asp(P_3) such that there is a favorable interaction with a negatively-charged residue such as Glu(192) of thrombin.

ACKNOWLEDGMENT

We thank Jean Lefebvre for peptide synthesis and purification and Bernard F. Gibbs for amino acid analysis.

REFERENCES

Blaney, J. M., Crippen, G. M., Dearing, A., & Dixon, J. S. (1990) *QCPE Bull. 10*, 37.

Cantor, C. R., & Schimmel, P. R. (1980) *Biophysical Chemistry*, W. H. Freeman and Co., San Francisco, CA.

Dahlbäck, B., Lundwall, A., Stebflo, J. (1986) *J. Biol. Chem. 261*, 5111.

Degen, S. J. F., MacGillivray, R. T. A., & Davie, E. W. (1983) *Biochemistry 22*, 2087.

DiMaio, J., Ni, F., Gibbs, B., & Konishi, Y. (1991) *FEBS Lett. 282*, 47.

Eaton, H. L., & Andersen, N. H. (1987) *J. Magn. Reson. 74*, 212.

Ehrlich, H. J., Grinnel, B. W., Jaskunas, S. R., Esmon, C. T., Yan, S. B., & Bang, N. U. (1990) *EMBO J. 9*, 2367.

Esmon, C. T. (1989) *J. Biol. Chem. 264*, 4743.
Fenton, J. W., II (1981) *Ann. N.Y. Acad. Sci. 370*, 468.
Fujikawa, K., Chung, D. W., Hendrickson, L. E., & Davie, E. W. (1986) *Biochemistry 25*, 2417.
Furlan, M. (1988) in *Fibrinogen, Fibrin Stabilization, and Fibrinolysis* (Francis, J. L., Ed.) pp 17–64, Ellis Horwood Ltd., Chichester, Great Britain.
Keepers, J. W., & James, T. L. (1984) *J. Magn. Reson. 57*, 404.
Ichinose, A., Hendrickson, L. E., Fujikawa, K., & Davie, E. W. (1986) *Biochemistry 25*, 6900.
Jardetzky, O., & Roberts, G. C. K. (1981) *NMR in Molecular Biology*, Academic Press, Orlando, FL.
Jenny, R. J., Pittman, D. D., Toole, J. J., Kriz, R. W., Aldape, R. A., Hewick, R. M., Kaufman, R. J., & Mann, K. G. (1987) *Proc. Natl. Acad. Sci. U.S.A. 84*, 4846.
Kisiel, W., & Davie, E. W. (1981) *Methods Enzymol. 80*, 320.
Laudano, A. W., & Doolittle, R. F. (1978) *Proc. Natl. Acad. Sci. U.S.A. 75*, 3085.
Le Bonniec, B. F., & Esmon, C. T. (1991) *Proc. Natl. Acad. Sci. U.S.A. 88*, 7371.
Le Bonniec, B. F., MacGillivray, R. T. A., & Esmon, C. T. (1991) *J. Biol. Chem. 266*, 13796.
Liu, L.-W., Vu, T.-K. H., Esmon, C. T., & Coughlin, S. R. (1991) *J. Biol. Chem. 266*, 16977.
MacGillivray, R. T. A., & Davie, E. W. (1984) *Biochemistry 23*, 1626.
Martin, P. D., Robertson, W., Turk, D., Huber, R., Bode, W., & Edwards, B. F. P. (1992) *J. Biol. Chem. 267*, 7911.
Naito, K., & Fujikawa, K. (1991) *J. Biol. Chem. 266*, 7353.
Ni, F. (1992a) *J. Magn. Reson. 96*, 651.
Ni, F. (1992b) *J. Magn. Reson. 99*, 391.
Ni, F., Konishi, Y., Frazier, R. B., Scheraga, H. A., & Lord, S. T. (1989a) *Biochemistry 28*, 3082.
Ni, F., Meinwald, Y. C., Vásquez, M., & Scheraga, H. A. (1989b) *Biochemistry 28*, 3094.
Ni, F., Konishi, Y., & Scheraga, H. A. (1990) *Biochemistry 29*, 4479.
Ni, F., Ripoll, D. R., Purisima, E. O. (1992) *Biochemistry 31*, 2545.
Olejniczak, E. T., Gampe, R. T., Jr., & Fesik, S. W. (1986) *J. Magn. Reson. 67*, 28.
Rasmussen, U. B., Vouret-Craviari, V., Jallat, S., Schlesinger, Y., Pages, G., Pavirani, A., Lecocq, J.-P., Pouyssegur, J., & Van Obberghen-Schilling, E. (1991) *FEBS Lett. 288*, 123.
Tropp, J. (1980) *J. Chem. Phys. 72*, 6035.
Vehar, G. A., Keyt, B., Eaton, D., Rodriquez, H., O'Brien, D. P., Rotblat, F., Oppermann, H., Keck, R., Wood, W. I., Harkins, R. N., Tuddenham, E. G. D., Lawn, R. M., & Capon, D. J. (1984) *Nature 312*, 337.
Vu, T.-K. H., Hung, D. T., Wheaton, V. I., & Coughlin, S. R. (1991a) *Cell 64*, 1057.
Vu, T.-K. H., Wheaton, V. I., Hung, D. T., Charo, I., & Coughlin, S. R. (1991b) *Nature 353*, 674.
Woessner, D. E. (1962) *J. Chem. Phys. 36*, 1.
Woessner, D. E. (1965) *J. Chem. Phys. 42*, 1855.
Wüthrich, K. (1986) *NMR of Proteins and Nucleic Acids*, Wiley & Sons, New York.
Zheng, Z., Ashton, R. W., Ni, F., & Scheraga, H. A. (1992) *Biochemistry 31*, 4426.